THE JOURNAL OF BIOLOGICAL CHEMISTRY
Vol. 276, No. 28, Issue of July 13, pp. 25791–25796, 2001

Printed in U.S.A.

Structural Determinants of Cold Adaptation and Stability in a Large Protein*

Received for publication, March 28, 2001
Published, JBC Papers in Press, April 26, 2001, DOI 10.1074/jbc.M102741200

Salvino D'Amico, Charles Gerday, and Georges Feller‡

From the Laboratory of Biochemistry, Institute of Chemistry B6, University of Liège, B-4000 Liège, Belgium

The heat-labile α-amylase from an antarctic bacterium is the largest known protein that unfolds reversibly according to a two-state transition as shown by differential scanning calorimetry. Mutants of this enzyme were produced, carrying additional weak interactions found in thermostable α-amylases. It is shown that single amino acid side chain substitutions can significantly modify the melting point T_m, the calorimetric enthalpy ΔH_{cal}, the cooperativity and reversibility of unfolding, the thermal inactivation rate constant, and the kinetic parameters k_{cat} and K_m. The correlation between thermal inactivation and unfolding reversibility displayed by the mutants also shows that stabilizing interactions increase the frequency of side reactions during refolding, leading to intramolecular mismatches or aggregations typical of large proteins. Although all mutations were located far from the active site, their overall trend is to decrease both k_{cat} and K_m by rigidifying the molecule and to protect mutants against thermal inactivation. The effects of these mutations indicate that the cold-adapted α-amylase has lost a large number of weak interactions during evolution to reach the required conformational plasticity for catalysis at low temperatures, thereby producing an enzyme close to the lowest stability allowing maintenance of the native conformation.

The cold-active and heat-labile α-amylase from the antarctic bacterium *Pseudoalteromonas haloplanktis* is an exceptional case because it is the largest known protein undergoing a reversible unfolding according to a two-state reaction pathway. It has been proposed that this unusual behavior is dictated by the requirement for an improved flexibility or plasticity of the protein molecule to perform catalysis at near-zero temperatures (1). Structural investigations have suggested that this is achieved by decreasing the number and strength of weak interactions stabilizing the native conformation (2–4). Accordingly, one can expect that any mutation designed to improve the stability of this fragile edifice will induce significant perturbations of the denaturation pattern, thereby giving evidence for the structural features linked to the unfolding parameters.

Small globular proteins that unfold according to a pure two-state process, *i.e.* reversibly and without a stable intermediate between the native and the unfolded states, have allowed researchers to establish the thermodynamic stability function accounting for the Gibbs energy change associated with their denaturation over physiological and nonphysiological temperature ranges. The current availability of this thermodynamic function, mainly gained by differential scanning calorimetry, represents much more than the simple physicochemical characterization of a polymer because it offers a powerful tool for investigation of the still unexplained "second genetic code," *i.e.* the driving force allowing a polypeptide to fold into a predetermined native and biologically active conformation (5). The validity of the bell-shaped stability curve, which predicts protein unfolding at both high and subzero temperatures, has been established by the experimental demonstration of cold unfolding (6). Proteins are said to be marginally stable because the positive Gibbs free energy change is only a small difference between the large enthalpic and entropic contributions in the temperature range restrained between the cold and hot melting temperatures. Basically, denaturation at high temperature is entropy-driven, because the large and positive thermal dissipative force exceeds the corresponding enthalpy change. By contrast, cold unfolding is enthalpy-driven and arises from the negative contribution of the hydration Gibbs energy of protein groups, mainly polar, at low temperatures (7).

Four parameters are usually assigned to the unfolding event recorded by differential scanning calorimetry, (i) the melting point of the unfolding transition; (ii) ΔCp, the difference in heat capacity between the native and unfolded states arising from the transfer of buried groups in the protein to water, in the random coil; (iii) ΔH_{cal}, the calorimetric enthalpy corresponding to the total amount of heat absorbed during unfolding and recorded by the calorimeter; and (iv) ΔH_{eff}, the effective or van't Hoff enthalpy calculated from the slope of the transition and describing the cooperativity of the unfolding reaction. In the case of a pure two-state model, ΔH_{cal} and ΔH_{eff} are nearly identical. However, large proteins generally unfold irreversibly as a result of strong heat-induced aggregation, with large deviations from the two-state model because their multidomain structure induces a stepwise or overlapping unfolding of domains, behaving as individual calorimetric units (Fig. 1).

We report here the calorimetric characterization of mutants from the cold-active α-amylase defined on the basis of its strong homology with heat-stable mesophilic α-amylases. These mutants reveal the unsuspected contribution of single amino acid substitutions to the thermodynamic parameters characteristic of large heat-stable proteins and provide new insight into the molecular adaptations of enzymes from psychrophilic organisms.

EXPERIMENTAL PROCEDURES

Mutagenesis and Protein Purification—Mutations in the *P. haloplanktis* α-amylase gene were introduced by polymerase chain reaction

* This work was supported by the European Community in the form of Network Contract CT970131, Biotech Program BIO4-CT96–0051, Région Wallonne-Direction Générale des Technologies Convention 1928, and Fonds National de la Recherche Scientifique Contract FRFC 2.4515.00. The costs of publication of this article were defrayed in part by the payment of page charges. This article must therefore be hereby marked "*advertisement*" in accordance with 18 U.S.C. Section 1734 solely to indicate this fact.

‡ To whom correspondence should be addressed: Laboratory of Biochemistry, Institute of Chemistry B6, University of Liège, B-4000 Liège, Belgium. Tel.: +32 4 366 33 43; Fax: +32 4 366 33 64; E-mail: gfeller@ulg.ac.be.

TABLE I
Selected mutations in this study

Mutants	Restored interactions[a]
K300R	Additional H-bond in the Cl^- binding site (A)
N150D	Salt bridge with Lys-190 (A)
V196F	Double aromatic interaction with Tyr-82 and Phe-198 (A)
N150D/V196F	Double mutant (A)
Q164I/V196F	Double mutant (A)
Q164I	Hydrophobic interaction in a core cluster (A)
T232V	Hydrophobic interaction in a core cluster (A)
N288V	Hydrophobic interaction in a core cluster (A)
M379V	Hydrophobic interaction in a core cluster (C)
R64E	Helix dipole stabilization (A)
L219R	Amino-aromatic interaction with Tyr-298 (A)
Del6	Deletion of 6 nonconstrained residues at the C terminus possibly involved in unzipping (C)
N12R	Salt bridge with Asp-15 (A)
E279W	Aromatic interaction with Phe-307 (A)

[a] (A) and (C) refer to the central $(\beta/\alpha)_8$ barrel and to the globular C-terminal domain, respectively.

as described (8). The nucleotide sequence of the constructions was checked on an Amersham Pharmacia Biotech ALF DNA sequencer. The recombinant wild-type α-amylase and the mutant enzymes were expressed in *Escherichia coli* at 18 °C and purified by DEAE-agarose, Sephadex G-100, and Ultrogel AcA54 column chromatography, as described previously (9). Pig pancreatic α-amylase (PPA)1 was from Roche.

Differential Scanning Calorimetry (DSC)—Measurements were performed using a MicroCal MCS-DSC instrument as detailed (1). Samples (~3 mg/ml) were dialyzed overnight against 30 mM MOPS, 50 mM NaCl, and 1 mM $CaCl_2$, pH 7.2. Thermograms were analyzed according to a non-two-state model in which T_m, ΔH_{cal}, and ΔH_{eff} of individual transitions are fitted independently using the MicroCal Origin software (version 2.9). The magnitude and source of the errors in the T_m and enthalpy values have been discussed elsewhere (10). Fitting standard errors on a series of three DSC measurements made under the same conditions in the present study were found to be ±0.05 K on T_m and ±1% on both enthalpies.

Thermal Inactivation—Thermograms generated by starch hydrolysis were recorded on a MCS isothermal titration calorimeter. The technical background for such an experiment has been described elsewhere (11). Starch concentration was 2% in 50 mM Hepes, 50 mM NaCl, 1 mM $CaCl_2$, pH 7.2, and was saturating during the time course of the experiment. Reactions were initiated by injecting 10–50 μl of a 30 μg/ml enzyme solution into the same buffer. The activity decay at 45 °C was recorded continuously for 30 min, and data were fitted on a monoexponential function to determine the first order constant rate of enzyme inactivation at 45 °C, S.E. <1%.

Enzyme Assay and Kinetics—The k_{cat} values were determined at 25 °C using 3.5 mM 4-nitrophenyl-α-D-maltoheptaoside-4,6-*O*-ethylidene as substrate (8). The k_{cat}/K_m values for substrate hydrolysis were determined from initial rates using the following relation. $k_{cat}/K_m = v_0/S_0E_0$, which is valid at $S_0 \ll K_m$ for systems that obey Michaelis-Menten kinetics. The validity of this equation was ascertained by performing determinations at three substrate concentrations.

RESULTS

Selection of Potentially Stabilizing Mutations—The psychrophilic α-amylase from *P. haloplanktis* (AHA) belongs to chloride-dependent α-amylases. This group includes all known animal α-amylases and the enzymes from some Gram-negative bacteria, covering a large range of living temperatures (12). The high degree of amino acid sequence identity between chloride-dependent α-amylases allowed us to construct a multiple sequence alignment of the available primary structures (12) and to detect about 20% of 453 residues that are specific to the cold-adapted enzyme. The involvement of these residues in the weak stability of the psychrophilic α-amylase was assessed by comparison of its crystal structure (3, 4) with that of PPA, the closest structural homolog, as well as with the structure of α-amylases from human salivary and pancreatic glands and from the insect *Tenebrio molitor*. Molecular modeling was then used to check the consistency of mutations aimed to introduce weak interactions found in mesophilic α-amylases in the heat-labile AHA. The selected mutations are listed in Table I along with the restored interactions. Following production in *E. coli* and purification, the stability and kinetic parameters of 14 mutant enzymes were determined (Table II). Mutants are listed according to their main properties, as discussed below. Fig. 1 depicts the microcalorimetric behavior of the recombinant wild-type AHA and of heat-stable α-amylases, including PPA taken as reference for mutation selection.

Enthalpic Stabilization by Electrostatic Interactions—Enthalpic stabilization involves an increase of the denaturation enthalpy and of the melting point. Such stabilization of the heat-labile α-amylase is obtained when a salt bridge (N150D), polar aromatic interactions (V196F), or an additional H-bond (K300R) is introduced in the protein. Thermal unfolding of some of these mutants is illustrated in Fig. 2. These additional electrostatic interactions induce a slightly higher T_m value (Table II) associated, however, with a large increase of the calorimetric enthalpy (ΔH_{cal}). Characterization of the double mutant N150D/V196F revealed several interesting features. The effect of the mutations on the melting point is additive (Table II, Fig. 2). Moreover, both mutations affect ΔH_{cal} and ΔH_{eff} differently, whereas their cumulative effect in the double mutant leads to a $\Delta H_{cal}/\Delta H_{eff}$ ratio at unity, indicative of a perfect two-state unfolding pattern.

Calorimetric Domain Acquirement by Nonpolar Groups—Aliphatic side chains were introduced in AHA in order to reconstruct hydrophobic core clusters found in mesophilic α-amylases (Q164I, T232V, N288V, and M379V). Interestingly, each substitution results in a non-two-state unfolding of the mutant enzymes and in the appearance of two calorimetric units or domains (Fig. 3). As also shown in Fig. 3, the separation between both calorimetric units in the mutants can be improved by adjusting the experimental conditions, providing evidence for the coexistence of two protein domains of distinct stability. Deconvolution of the heat capacity function revealed that one domain always has an increased T_m compared with that of AHA (Table II), underlining the stabilization induced by the reconstituted hydrophobic cluster. By contrast, the lower T_m of the first domain seems to be the consequence of strain imposed in one domain that is not compensated in other protein regions. This is supported by the combination of mutations Q164I and V196F resulting in a mutant enzyme displaying two stabilized domains, as far as T_m is concerned. The mutant T232V deserves special comments. Indeed, the shape of its heat capacity

[1] The abbreviations used are: PPA, pig pancreatic α-amylase; AHA, *P. haloplanktis* α-amylase; BAA, *B. amyloliquefaciens* α-amylase; DSC, differential scanning calorimetry.

TABLE II
Stability and kinetic parameters of wild-type and mutant α-amylases

	T_m	ΔH_{cal}	ΔH_{eff}	$\Delta H_{cal}/\Delta H_{eff}$	Reversibility	k_{inact}	k_{cat}	K_m	k_{cat}/K_m
	°C	*kcal mol^{-1}*	*kcal mol^{-1}*		*%*	*10^{-3} s^{-1}*	*s^{-1}*	*μM*	*s^{-1} μM^{-1}*
Heat-labile α-amylase									
AHA	44.0	214	203	1.05	100	2.27	697 ± 33	234 ± 18	2.98
Enthalpic stabilization									
K300R	45.2	223	217	1.03	87	0.59	326 ± 17	141 ± 2	2.31
N150D	44.8	271	240	1.13	97	1.53	682 ± 31	241 ± 10	2.83
V196F	45.4	234	296	0.79	60	0.95	752 ± 5	223 ± 12	3.37
N150D/V196F	46.4	272	271	1	91	0.54	642 ± 25	174 ± 11	3.69
Calorimetric domains									
Q164I/V196F									
(1)[a]	44.7	83	121	0.69	51	0.87	501 ± 12	153 ± 7	3.27
(2)	46.2	125	308	0.41					
Q164I									
(1)	42.7	87	117	0.74	64	1.77	514 ± 18	118 ± 11	4.36
(2)	45.2	117	240	0.49					
T232V									
(1)	42.7	102	114	0.89	85	2.51	735 ± 16	164 ± 22	4.48
(2)	45.7	104	202	0.51					
N288V									
(1)	38.1	88	133	0.66	30		350 ± 14	139 ± 7	2.52
(2)	45.9	59	114	0.52					
M379V									
(1)	42.6	127	96	1.32	95	2.25	633 ± 24	159 ± 4	3.98
(2)	47.7	84	137	0.61					
Unfolding cooperativity									
R64E	42.6	236	112	2.11	96	2.22	719 ± 6	220 ± 24	3.27
L219R	42.5	217	187	1.16	81	1.17	469 ± 42	144 ± 3	3.26
Del6	42.4	211	285	0.74	89	2.07	726 ± 21	264 ± 7	2.75
N12R	43.3	193	231	0.84	25	2.48	670 ± 27	178 ± 6	3.76
E279W	41.4	186	234	0.79	76	2.40	744 ± 22	201 ± 14	3.70
Heat-stable α-amylase									
PPA									
(1)	61.7	147	127	1.16	0	0	291 ± 8	65 ± 4	4.48
(2)	65.6	148	246	0.6					

[a] (1) and (2) refer to calorimetric domains identified by deconvolution of DSC thermograms.

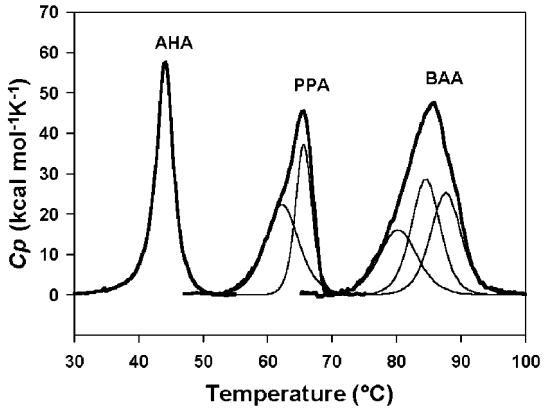

FIG. 1. **Thermal unfolding of α-amylases recorded by DSC.** The heat-stable PPA and BAA are characterized by higher T_m (*top of the transition*) and ΔH_{cal} (*area under the transition*) values, by a flattening of the transition and by the occurrence of calorimetric domains (deconvolutions are in *thin lines*). All thermograms are base line-subtracted and normalized for protein concentrations.

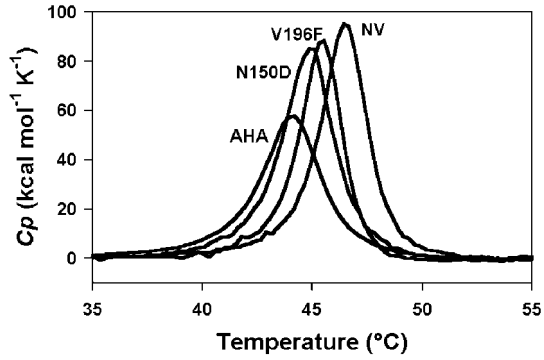

FIG. 2. **Enthalpic stabilization.** Thermal unfolding of AHA and of single and double mutants (*NV*, N150D/V196F) characterized by increased T_m and ΔH_{cal} values.

function is similar to that of PPA (Fig. 3) as well as the relative contribution of each domain to ΔH_{cal} and ΔH_{eff} (Table II). Therefore, this mutant consistently reproduces the microcalorimetric unfolding pattern of the heat-stable PPA but at lower temperatures.

Cooperativity of Unfolding—The comparison of ΔH_{cal} and ΔH_{eff} values allows us to analyze the unfolding cooperativity by microcalorimetry. Several mutations listed in Table II affect the unfolding cooperativity without noticeable change of ΔH_{cal}. Thermal unfolding of mutants Del6, L219R and R64E (Fig. 4) clearly illustrates the relation between ΔH_{eff} and the steepness of the transition. Furthermore, the thermogram slope of mutants L219R and R64E is considerably decreased and approaches the profile of large and stable proteins such as *Bacillus amyloliquefaciens* α-amylase (BAA) (Fig. 1).

Folding and Unfolding Reversibility—In these experiments, the mutant enzymes were 100% unfolded, then allowed to refold during a cooling period of 15 min at 15 °C. Reversibility was calculated by the recovery of ΔH_{cal} during a second scan (Table II). Substitution of a single amino acid side chain is sufficient to drastically alter this critical parameter of protein folding, as demonstrated by mutant N12R that displays only 25% renaturation. Mutants Q164I, V196F, and Q164I/V196F that are stabilized by hydrophobic groups also decrease the unfolding reversibility significantly. In the same conditions, unfolding of the heat-stable PPA and BAA is completely irreversible.

Thermal Inactivation Recorded by Isothermal Titration Calorimetry—Determination of inactivation rate constants usually requires the recording of the residual enzyme activity after

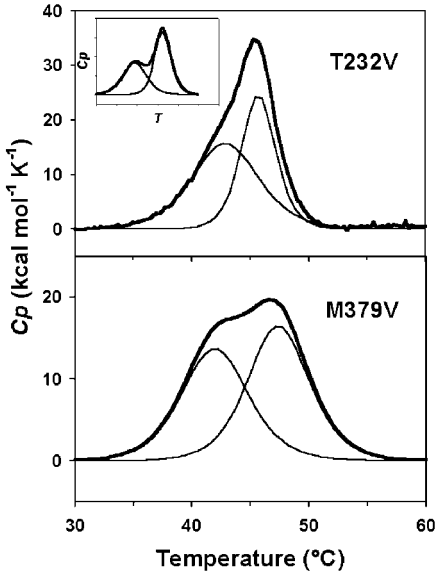

FIG. 3. **Calorimetric domains induced by additional nonpolar groups in hydrophobic core clusters (*inset*, T232V, pH 8.0).**

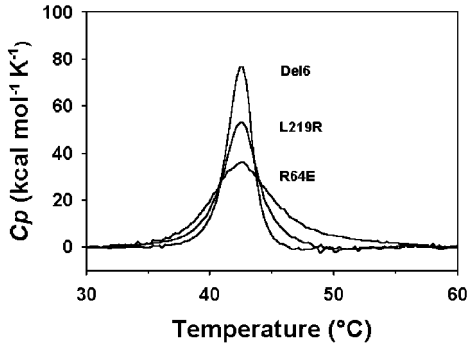

FIG. 4. **Alteration of unfolding cooperativity.** Decreasing the steepness of the transition maintains a higher level of native structures at elevated temperatures.

incubation at high temperature. In the case of AHA and of its mutants, the model of Lumry and Eyring (13) is valid:

$$N \underset{k_{-1}}{\overset{k_1}{\rightleftharpoons}} U \xrightarrow{k_2} I \qquad \text{(Eq. 1)}$$

where k_2 is the first order rate constant of thermal inactivation. However, the various degrees of reversibility noted for the mutants (kinetically characterized by k_{-1}) strongly impair the validity of the results obtained by conventional methods. We have therefore devised a new method using isothermal titration calorimetry and recording activity at 45 °C as the heat released by the hydrolysis of starch glycosidic bonds. This method provides a direct and continuous monitoring of activity at the denaturing temperature (Fig. 5). As a prerequisite, the same experiment was followed by fluorescence (without substrate) showing that the structural modifications accompanying a temperature shift from 15 to 45 °C are fast with a k_1 value of about 0.04 s^{-1}. Therefore, the transition N → U is one order of magnitude faster than the transition U → I, and the disappearance of the active state N can be taken as a measure of k_2, as reported in Table II. It is significant that 10 of 14 mutants are protected against thermal inactivation and that mutants carrying newly introduced electrostatic interactions display the lowest inactivation rate constants (Fig. 5). A plot of unfolding reversibility *versus* thermal inactivation (Fig. 6*A*) shows that these parameters

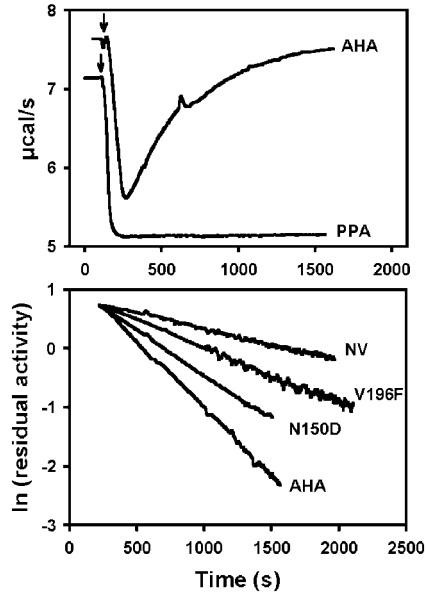

FIG. 5. **Thermal inactivation recorded by isothermal titration calorimetry.** *Upper panel*, following enzyme injection (*arrow*), activity at 45 °C is recorded as the heat flow of the reaction. Note the stability of PPA and the activity decay of AHA. *Lower panel*, semilogarithmic plot of residual activity *versus* time illustrating the lower inactivation rate of some mutants. *NV*, N150D/V196F.

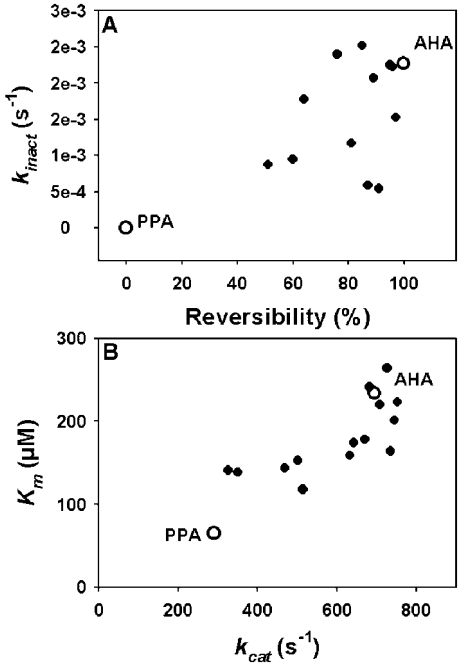

FIG. 6. **Correlation of stability (*A*) and kinetic (*B*) parameters for wild-type (○) and mutant (●) α-amylases.**

for the mutant enzymes are clustered between the respective values for AHA and PPA.

Kinetic Parameters—The kinetic parameters k_{cat} and K_m were recorded using a chromogenic maltoheptaose oligosaccharide (Table II). From these results, four main aspects should be pointed out. (i) As reported previously, AHA possesses a higher activity (k_{cat}) than PPA in order to compensate for the slow chemical reaction rates at low temperature. (ii) The general trend of the mutations is to decrease both k_{cat} and K_m. Fig. 6*B* shows that both kinetic parameters for mutants all fall within a narrow region of the plot, between the values of AHA and PPA. (iii) As a result, the mutations tend to raise the specificity constant or catalytic efficiency k_{cat}/K_m to values close to that of

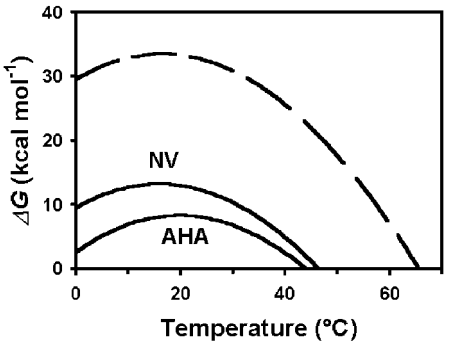

FIG. 7. **Stability curves of AHA and of the double mutant N150D/V196F (*NV*).** *Dashed line*, theoretical curve for a heat-stable α-amylase, using data from Ref. 41.

PPA (Table II). (iv) Most mutations protecting the enzymes against thermal inactivation also concomitantly decrease the k_{cat} value.

DISCUSSION

Stability of Large Proteins—The magnitude of the contribution, as recorded by microcalorimetry, of a single amino acid side chain to the stability parameters of a large protein is one of the most significant features revealed by engineering the heat-labile α-amylase. Such individual contributions are generally masked in stable proteins by the complex network of interactions involved in the native state conformation and by the fact that frequently, heat-induced unfolding of large proteins is kinetically driven as a result of pronounced irreversibility. Our results show that the selected electrostatic interactions provide the largest contribution to stability *per se*, by increasing both T_m and ΔH_{cal} and by protecting mutants against thermal inactivation (Table II). Thermal unfolding of the double mutant N150D/V196F follows the two-state transition model and is essentially reversible. Accordingly, its thermodynamic stability can be analyzed using the modified Gibbs-Helmholtz equation:

$$\Delta G(T) = \Delta H_m(1 - T/T_m) + \Delta Cp(T - T_m) - T\Delta Cp \ln (T/T_m) \quad \text{(Eq. 2)}$$

This function corresponds to the energy required to disrupt the native state (14) and is illustrated in Fig. 7. One can note that despite a modest increase of the melting point, the conformational energy of the double mutant is twice that of the wild-type AHA around 10 °C. Similarly, the contribution at 20 °C of the ion pair in N150D can be estimated to 4.4 kcal/mol, of the H-bond in K300R to 0.7 kcal/mol, and of a polar aromatic interaction in V196F (assuming two interplanar interactions) to 0.8 kcal/mol. These values are in good agreement with data obtained by *ab initio* calculations (15) or by experimental studies (16, 17). These free energy gains originate, however, from very large enthalpic-entropic compensation effects. The denaturation enthalpy and entropy can be calculated according to the relations (18):

$$\Delta H(T) = \Delta H_m + \Delta Cp(T - T_m) \quad \text{(Eq. 3)}$$

$$\Delta S(T) = \Delta H_m/T_m + \Delta Cp \ln (T/T_m) \quad \text{(Eq. 4)}$$

For instance, the denaturation enthalpy at 20 °C for AHA is 10.5 kcal/mol, and the entropic term ($T\Delta S$) amounts to 2.2 kcal/mol. The corresponding values for mutant N150D are 60.9 and 48.2 kcal/mol, respectively. Therefore, the gain of 4.4 kcal/mol in conformational energy provided by the ion pair arises from a 6-fold increase of the denaturation enthalpy balanced by a 20-fold increase of the entropic cost. It should be added that mutant N150D restores a surface salt bridge. Although the net contribution of solvent-exposed ion pairs has been frequently questioned (19), our results demonstrate that such interactions can provide a substantial increment of conformational stability. This is especially relevant for thermophilic and hyperthermophilic proteins that are characterized by an abundance of surface ion pairs (20), in some instances organized in interconnected networks (21, 22). On the other hand, about 8 ion pairs, 15 arginine residues and 10 aromatic interactions are lacking in the crystal structure of AHA when compared with the heat-stable PPA (3). The disappearance of these electrostatic based features is obviously a main determinant for both the low T_m and melting enthalpy of the psychrophilic α-amylase.

It is generally agreed that the hydrophobic effect is the main factor in stabilizing folded conformations (23). As shown in Fig. 3 and Table II, the insertion of a nonpolar group into a hydrophobic core cluster creates a stabilization center in the protein and in the peculiar case of AHA promotes the appearance of calorimetric domains. Unfortunately, large deviations from the two-state model preclude any reliable calculation for these mutants. It should be noted, however, that the increases of T_m for the stabilized transition are of the same magnitude or even higher (M379V) than that provided by electrostatic interactions. Analysis of the hydrophobic clusters in AHA shows that 20 substitutions decrease the hydrophobicity index of the involved residues relative to PPA. As indicated by the calorimetric behavior of the mutations selected for this work (Fig. 3), the overall low core hydrophobicity of the heat-labile AHA accounts to a large extent for the lack of discrete unfolding intermediates. It is usually accepted that extreme cooperativity is only achieved in small molecules with tight packing of groups (14). This obviously is not the case for the large multidomain heat-labile α-amylase. As suggested by the mutation effects, its unfolding cooperativity arises from the very low number of interactions maintaining the native state, which therefore results in the simultaneous disruption of all structural elements and in the unusual two-state unfolding of this large protein. Considering protein adaptation to temperature, a practical implication of the flattening of the unfolding transition in thermostable α-amylases such as BAA (Fig. 1) is to maintain a higher level of native conformation at elevated temperatures. Fig. 4 shows that the same holds true between 45 and 55 °C for mutants of the heat-labile α-amylase with altered cooperativity. The relation between unfolding reversibility and thermal inactivation (Fig. 6*A*) is another unsuspected result gained from the α-amylase mutant analysis. Referring to Equation 1, mutants protected against thermal inactivation are also those that refold less efficiently, mimicking the behavior of thermostable α-amylases. This could be explained by the large number of all types of weak interactions required for proper folding and stability in mesophilic and thermophilic enzymes. As a consequence, there will be more possibilities of side reactions during refolding, either by intramolecular mismatch or by aggregation due to replacement of the regular intramolecular pairing by intermolecular interactions (17).

Cold Adaptation—It was shown that all 24 side chains in the active site performing H-bonding to a large pseudosaccharide inhibitor in the transition state conformation are strictly conserved in both AHA and PPA crystal structures (4, 24). As a consequence, changes in primary structure that occur far from the active site should be responsible for the high specific activity of AHA. As a matter of fact, all mutations in this study designed to restore a mesophilic character are located far from the catalytic center and tend to decrease both k_{cat} and K_m (Fig. 6*B*). It has been convincingly argued that increases in flexibil-

ity of cold-adapted enzymes lead to a broader distribution of conformational states, translated into higher K_m values for enzymes devoid of adaptive changes within the active site (25, 26). In this context, rigidifying the molecule or part of the molecule by the newly engineered weak interactions in the psychrophilic α-amylase should contribute to decreased K_m values by reducing the conformational entropy of the binding-competent species. The kinetic parameters of the mutants (Fig. 6*B*) give experimental support to the previous hypothesis that temperature-adaptive increases in k_{cat} occur concomitantly with increases in K_m (26).

It has been proposed that stability and activity are not physically linked (27). Laboratory evolution can indeed yield non-natural catalysts that are thermostable and active either at high (28) or low (29, 30) temperatures. Nevertheless, when the selection is only applied on low temperature activity (the relevant parameter for psychrophilic enzymes), especially by *in vivo* functional selection systems (allowing cell growth, for instance), the evolved enzymes generally display a concomitant reduced thermostability (31–34). It was assumed that the selective advantage for these optimized catalysts depends on a high k_{cat} and not on maintaining stability (27). However, our structure-based approach demonstrates that natural mutations occurring in the cold-active α-amylase associate high activity and low stability. The convergence of the results from both random and rational studies stresses that the lack of selective pressure for stable proteins at low temperatures does not entirely account for the instability of psychrophilic proteins. On the contrary, heat lability or conformational plasticity seems to be intimately interlaced with sustained activity in cold environments. This is possibly the easiest route taken by natural selection on the evolutionary time scale or because large fluctuations around the native state are required by the energetics of substrate binding (35) and catalysis at low temperatures, an aspect that is not documented for such enzymes to date. The mutant N288V represents an extreme case. This mutant possesses a heat-labile domain with the lowest T_m (Table II) but is marginally stable even at 4 °C, with a half-life of 2 h at 25 °C and requiring fast purification procedures. This behavior is consistent with the proposal that AHA has reached a state close to the lowest accessible stability of its native state and cannot be further destabilized (1). If indeed stability is linked to activity in cold-adapted enzymes, this limitation explains the imperfect adaptation of psychrophilic enzymes, *i.e.* their activity at low temperatures remains lower than that of mesophiles at 37 °C.

Concluding Remarks—This mutational analysis of a large protein demonstrates that the psychrophilic α-amylase has lost numerous weak interactions during evolution to reach the proper conformational flexibility at low temperatures. These adaptive adjustments contribute to improve k_{cat} without alteration of the catalytic mechanism, because the active site architecture is not modified, but at the expense of a weaker substrate binding affinity. On the other hand, thermophilic enzymes strengthen the same type of interaction to gain in structural stability at high temperatures but at the expense of poor activity at room temperature (36–38). These aspects underline the continuum in the strategy of temperature adaptation in proteins and reinforce the concepts of "compromise" (39) between activity and stability leading to "corresponding states" (40) of enzymes adapted to different thermal environments.

Acknowledgments—We thank N. Gérardin and R. Marchand for their skillful technical assistance.

REFERENCES

1. Feller, G., d'Amico, D., and Gerday, C. (1999) *Biochemistry* **38,** 4613–4619
2. Feller, G., Payan, F., Theys, F., Qian, M., Haser, R., and Gerday, C. (1994) *Eur. J. Biochem.* **222,** 441–447
3. Aghajari, N., Feller, G., Gerday, C., and Haser, R. (1998) *Structure* **6,** 1503–1516
4. Aghajari, N., Feller, G., Gerday, C., and Haser, R. (1998) *Protein Sci.* **7,** 564–572
5. Rumbley, J., Hoang, L., Mayne, L., and Englander, S. W. (2001) *Proc. Natl. Acad. Sci. U. S. A.* **98,** 105–112
6. Privalov, P. L. (1990) *Crit. Rev. Biochem. Mol. Biol.* **25,** 281–305
7. Makhatadze, G. I., and Privalov, P. L. (1995) *Adv. Protein. Chem.* **47,** 307–425
8. Feller, G., le Bussy, O., Houssier, C., and Gerday, C. (1996) *J. Biol. Chem.* **271,** 23836–23841
9. Feller, G., le Bussy, O., and Gerday, C. (1998) *Appl. Environ. Microbiol.* **64,** 1163–1165
10. Matouschek, A., Matthews, J. M., Johnson, C. M., and Fersht, A. R. (1994) *Protein Eng.* **7,** 1089–1095
11. Lonhienne, T., Baise, E., Feller, G., Bouriotis, V., and Gerday, C. (2001) *Biochim. Biophys. Acta* **1545,** 349–356
12. D'Amico, S., Gerday, C., and Feller, G. (2000) *Gene* (*Amst.*) **253,** 95–105
13. Lumry, R., and Eyring, H. (1954) *J. Phys. Chem.* **58,** 110–120
14. Privalov, P. (1992) in *Protein Folding* (Creighton, T., ed) pp. 83–126, W. H. Freeman and Company, New York
15. Burley, S. K., and Petsko, G. A. (1988) *Adv. Protein. Chem.* **39,** 125–189
16. Anderson, D. E., Becktel, W. J., and Dahlquist, F. W. (1990) *Biochemistry* **29,** 2403–2408
17. Jaenicke, R. (1999) *Prog. Biophys. Mol. Biol.* **71,** 155–241
18. Privalov, P. L. (1979) *Adv. Protein. Chem.* **33,** 167–241
19. Strop, P., and Mayo, S. L. (2000) *Biochemistry* **39,** 1251–1255
20. Cambillau, C., and Claverie, J. M. (2000) *J. Biol. Chem.* **275,** 32383–32386
21. Pappenberger, G., Schurig, H., and Jaenicke, R. (1997) *J. Mol. Biol.* **274,** 676–683
22. Vetriani, C., Maeder, D. L., Tolliday, N., Yip, K. S., Stillman, T. J., Britton, K. L., Rice, D. W., Klump, H. H., and Robb, F. T. (1998) *Proc. Natl. Acad. Sci. U. S. A.* **95,** 12300–12305
23. Matthews, B. W. (1993) *Annu. Rev. Biochem.* **62,** 139–160
24. Qian, M., Haser, R., Buisson, G., Duee, E., and Payan, F. (1994) *Biochemistry* **33,** 6284–6294
25. Holland, L. Z., McFall-Ngai, M., and Somero, G. N. (1997) *Biochemistry* **36,** 3207–3215
26. Fields, P. A., and Somero, G. N. (1998) *Proc. Natl. Acad. Sci. U. S. A.* **95,** 11476–11481
27. Petrounia, I. P., and Arnold, F. H. (2000) *Curr. Opin. Biotechnol.* **11,** 325–330
28. Cherry, J. R., Lamsa, M. H., Schneider, P., Vind, J., Svendsen, A., Jones, A., and Pedersen, A. H. (1999) *Nat. Biotechnol.* **17,** 379–384
29. Giver, L., Gershenson, A., Freskgard, P. O., and Arnold, F. H. (1998) *Proc. Natl. Acad. Sci. U. S. A.* **95,** 12809–12813
30. Miyazaki, K., Wintrode, P. L., Grayling, R. A., Rubingh, D. N., and Arnold, F. H. (2000) *J. Mol. Biol.* **297,** 1015–1026
31. Lebbink, J. H., Kaper, T., Bron, P., van der Oost, J., and de Vos, W. M. (2000) *Biochemistry* **39,** 3656–3665
32. Merz, A., Yee, M. C., Szadkowski, H., Pappenberger, G., Crameri, A., Stemmer, W. P., Yanofsky, C., and Kirschner, K. (2000) *Biochemistry* **39,** 880–889
33. Wintrode, P. L., Miyazaki, K., and Arnold, F. H. (2000) *J. Biol. Chem.* **275,** 31635–31640
34. Roovers, M., Sanchez, R., Legrain, C., and Glansdorff, N. (2001) *J. Bacteriol.* **183,** 1101–1105
35. Ma, B., Kumar, S., Tsai, C. J., and Nussinov, R. (1999) *Protein Eng.* **12,** 713–720
36. Varley, P. G., and Pain, R. H. (1991) *J. Mol. Biol.* **220,** 531–538
37. Zavodszky, P., Kardos, J., Svingor, A., and Petsko, G. A. (1998) *Proc. Natl. Acad. Sci. U. S. A.* **95,** 7406–7411
38. Kohen, A., Cannio, R., Bartolucci, S., and Klinman, J. P. (1999) *Nature* **399,** 496–499
39. Somero, G. N. (1995) *Annu. Rev. Physiol.* **57,** 43–68
40. Jaenicke, R., and Bohm, G. (1998) *Curr. Opin. Struct. Biol.* **8,** 738–748
41. Fukada, H., Takahashi, K., and Sturtevant, J. M. (1987) *Biochemistry* **26,** 4063–4068